Biochemistry and Biophysics Reports 4 (2015) 357–368

Contents lists available at ScienceDirect

Biochemistry and Biophysics Reports

journal homepage: www.elsevier.com/locate/bbrep

Novel curcumin derivatives as potent inhibitors of amyloid β aggregation

Daijiro Yanagisawa [a], Hiroyasu Taguchi [a], Shigehiro Morikawa [a], Tomoko Kato [a], Koichi Hirao [b], Nobuaki Shirai [c], Ikuo Tooyama [a,*]

[a] Molecular Neuroscience Research Center, Shiga University of Medical Science, Seta Tsukinowa-cho, Otsu 520-2192, Japan
[b] Northeastern Industrial Research Center of Shiga Prefecture, 27-39 Mitsuya Motomachi, Nagahama 526-0024, Japan
[c] Industrial Research Center of Shiga Prefecture, 232 Kamitoyama, Ritto 520-3004, Japan

ARTICLE INFO

Article history:
Received 6 July 2015
Received in revised form
21 October 2015
Accepted 23 October 2015
Available online 26 October 2015

Keywords:
Alzheimer's disease
Amyloid β
Aggregation
Curcumin

ABSTRACT

Modulation of abnormal amyloid β (Aβ) aggregation is considered to be a potential therapeutic target for Alzheimer's disease (AD). Recent *in vitro* and *in vivo* experiments suggest that inhibition of Aβ aggregation by curcumin would exert favorable effects for preventing or treating AD. We have previously synthesized a series of novel curcumin derivatives. In this study, we investigated the effects of our curcumin derivatives on Aβ aggregation and the cell toxicities of Aβ aggregates. According to sodium dodecyl sulfate polyacrylamide gel electrophoresis (SDS-PAGE) profiles, 14 of 41 compounds showed a significant increase in the densities of the bands of Aβ (1–42) by incubation during the aggregation process relative to those of Aβ (1–42) prepared in the presence of the vehicle control. Of the 14 compounds, four compounds additionally reduced cell toxicity of the Aβ aggregates by incubation during the aggregation process. A significant positive correlation was observed between the cell viability and densities of the bands at ranges of 15–20, 20–37, 37–75, and 75–200 kDa in SDS-PAGE. On the basis of these results, we propose four curcumin derivatives with potential for preventing AD. These curcumin derivatives exhibited high inhibitory effects on Aβ aggregation and induced the formation of lower molecular size Aβ species that have weaker cell toxicity. These compounds may exert therapeutic effects on AD in future *in vivo* studies.

© 2015 The Authors. Published by Elsevier B.V. This is an open access article under the CC BY-NC-ND license (http://creativecommons.org/licenses/by-nc-nd/4.0/).

1. Introduction

Alzheimer's disease (AD) is characterized by a progression from episodic memory difficulties to a slow global decline in cognitive function [1,2]. Recent studies on the progression of AD strongly support the amyloid cascade hypothesis that a pathological change in amyloid β (Aβ) in the brain is an initiating event in AD [3,4]. Aβ is normally and ubiquitously expressed throughout life as peptides of mainly 40 and 42 residues. By unknown mechanisms, monomeric Aβ polymerizes, forms long insoluble fibrillar aggregates, and accumulates in extracellular deposits known as senile plaques. Such abnormal aggregates of Aβ are believed to induce hyperphosphorylation of tau, tangle formation, and neuronal loss, which eventually results in cognitive impairment. Accordingly, modulation of abnormal Aβ aggregation is considered to be a potential therapeutic target for AD.

Curcumin, a polyphenol, is a low-molecular weight yellow-orange pigment derived from the well-known curry spice turmeric, obtained from the rhizome of *Curcuma longa*. Curcumin may have numerous biochemical and molecular targets, including transcription factors, inflammatory cytokines, enzymes, kinases, growth factors, receptors, adhesion molecules, and anti-apoptosis proteins, as described in the review by Goel et al. [5]. In addition, recent *in vitro* and *in vivo* experiments suggest that the inhibitory effect of curcumin on Aβ aggregation would be favorable for preventing or treating AD [6–12].

We recently reported a novel curcumin derivative, 1,7-bis (4′-hydroxy-3′-trifluoromethoxyphenyl)-4-methoxycarbonylethyl-1,6-heptadiene-3,5-dione (FMeC1), as a fluorine-19 magnetic resonance imaging (MRI) probe to detect amyloid deposition in the brain [13–15]. FMeC1 penetrated the blood–brain barrier and bound to amyloid plaques in a transgenic mouse model of AD after injection *via* the tail vein. Because FMeC1 has six atoms of fluorine in its structure, FMeC1 accumulation can be detected in the mouse brain using fluorine-19 MRI. Treatment of FMeC1 has been shown to inhibit cognitive decline and reduce amyloid deposition in APP/PS1 mice, which suggests a therapeutic potential of FMeC1 for preventing AD [16]. FMeC1 has been shown to inhibit the

* Corresponding author. Fax: +81 77 548 2331.
E-mail address: kinchan@belle.shiga-med.ac.jp (I. Tooyama).

http://dx.doi.org/10.1016/j.bbrep.2015.10.009
2405-5808/© 2015 The Authors. Published by Elsevier B.V. This is an open access article under the CC BY-NC-ND license (http://creativecommons.org/licenses/by-nc-nd/4.0/).

Table 1
Structures of curcumin and its derivatives

Name	Structure	MW	*C* log *P*	IC_{50} (μM)
Cur	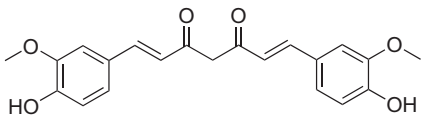	368.38	2.56	0.20
MR195	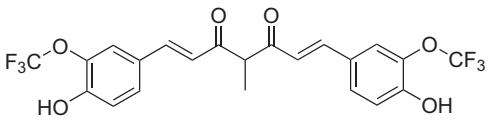	490.35	6.43	0.32
SY1	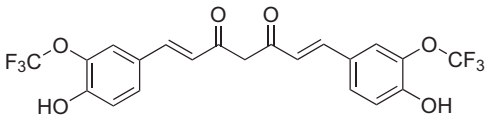	476.32	5.87	0.26
SY2	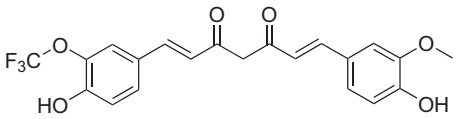	422.35	4.21	N.D.
SY4	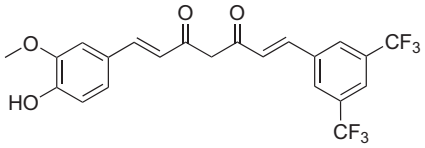	458.35	4.92	N.D.
SY5	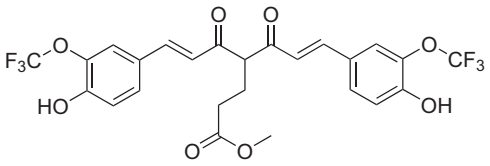	562.41	6.13	0.44
SY6	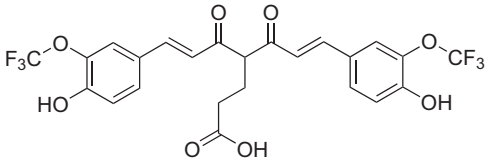	548.38	5.87	0.82
SY7	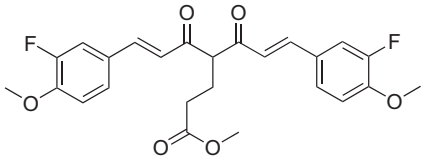	458.45	3.92	N.D.
SY8	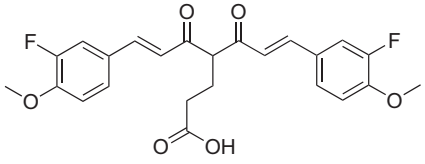	444.42	3.65	N.D.
SY9	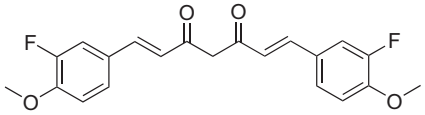	372.36	3.66	N.D.
SY10	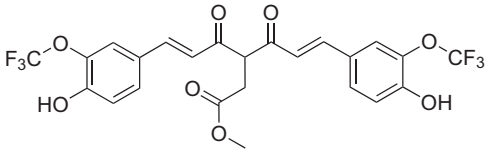	548.39	5.71	0.57
SY11	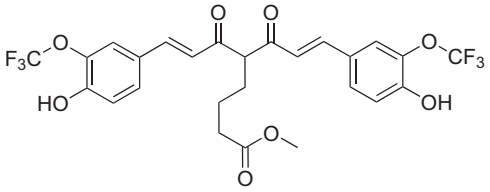	576.44	6.55	0.35

Table 1 (*continued*)

Name	Structure	MW	*C* log *P*	IC_{50} (μM)
SY12	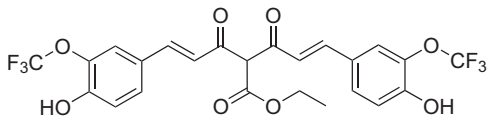	548.39	6.11	0.13
SY13	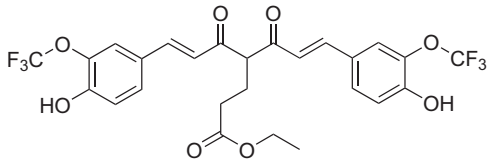	576.44	6.47	0.38
SY14	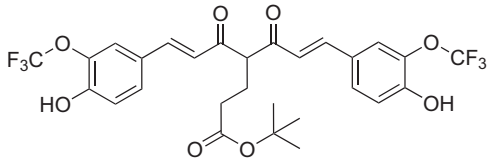	604.49	7.00	0.65
SY15	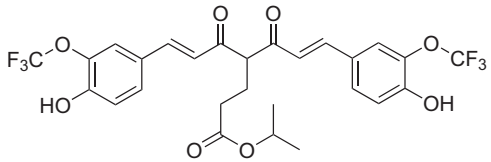	590.47	6.79	0.39
SY16	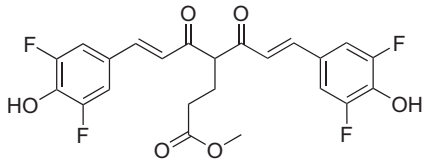	466.38	3.71	0.59
SY17	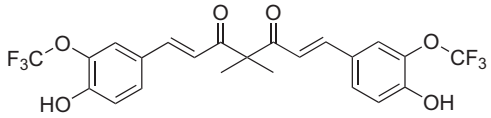	504.38	7.14	10.16
SY18	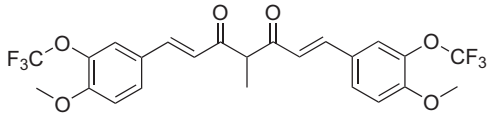	518.4	6.96	16.20
SY20	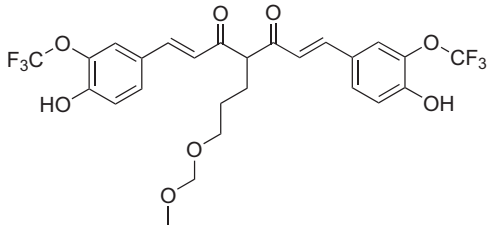	578.45	6.55	0.50
SY21	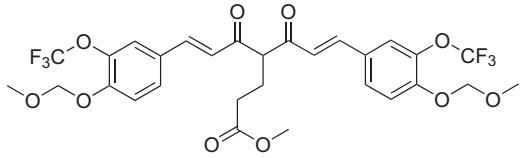	650.52	6.90	4.71
SY22	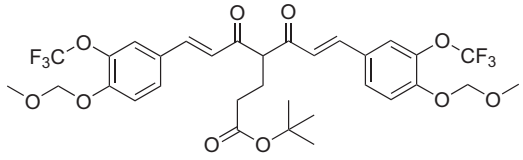	692.6	7.77	20.30
SY23	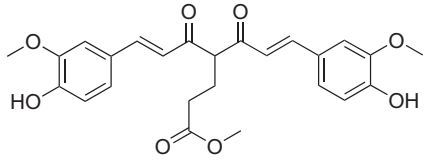	454.47	2.82	0.32

Table 1 (*continued*)

Name	Structure	MW	*C* log *P*	IC_{50} (μM)
SY26	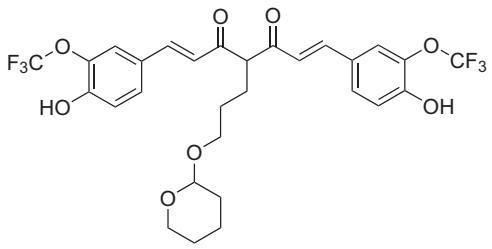	618.52	7.28	0.31
SY27	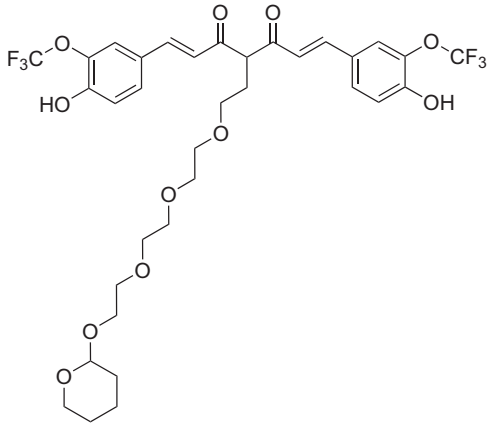	736.65	6.39	0.93
SY28	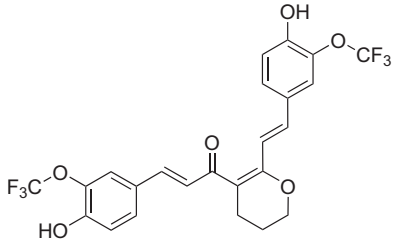	516.1	6.09	1.23
SY29	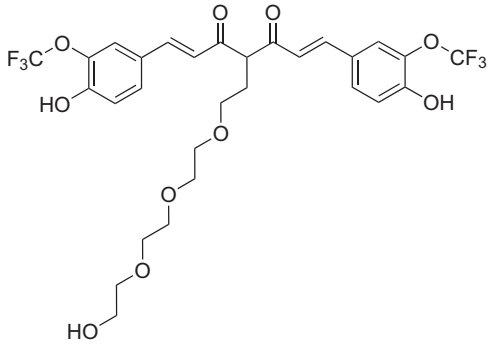	652.53	5.19	1.85
SY30	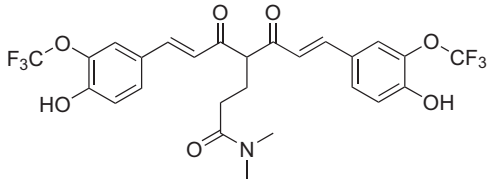	575.45	5.69	0.50
SY31	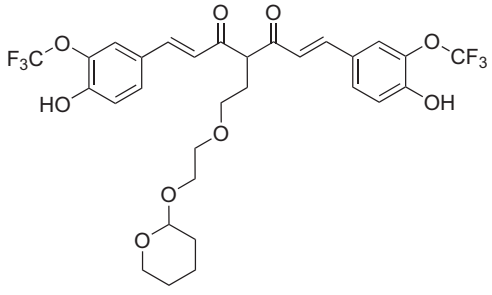	648.54	6.00	0.65

Table 1 (*continued*)

Name	Structure	MW	*C* log *P*	IC_{50} (μM)
SY32	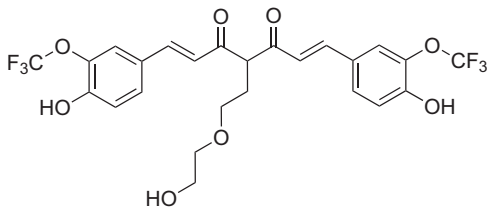	564.43	5.50	0.70
SY33	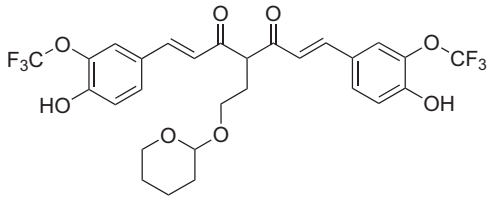	604.49	6.15	0.57
SY34	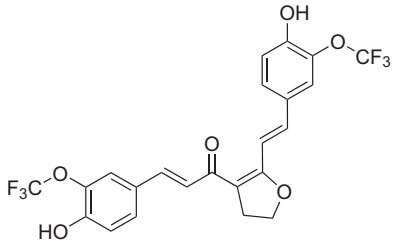	502.36	5.68	0.25
SY35	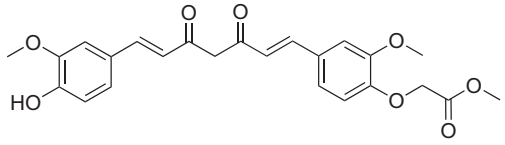	440.44	2.35	0.14
SY36	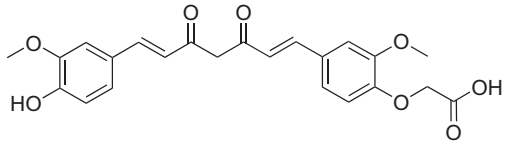	426.42	2.09	0.31
SY37	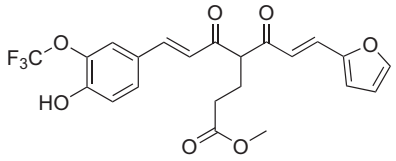	452.38	3.61	0.65
SY38	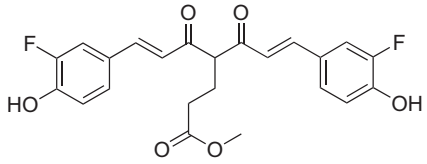	430.4	3.39	N.D.
SY39	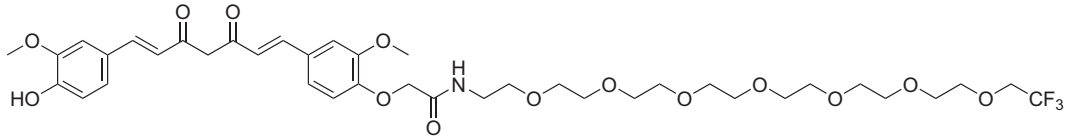	815.82	–	N.D.
SY40	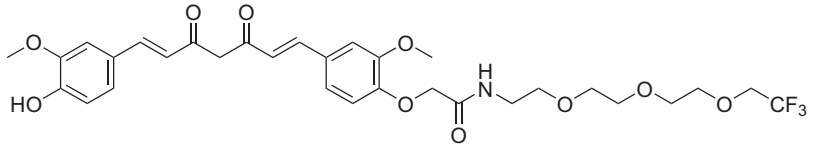	639.61	2.19	N.D.
SY41	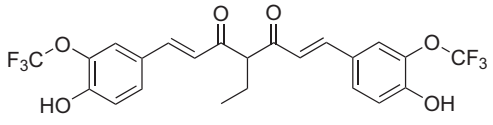	504.38	6.85	N.D.

Table 1 (*continued*)

Name	Structure	MW	*C* log *P*	IC_{50} (μM)
SY42	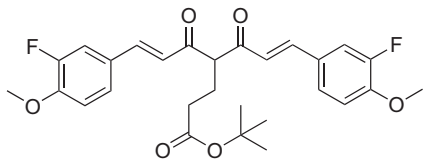	500.53	4.79	N.D.
SY43	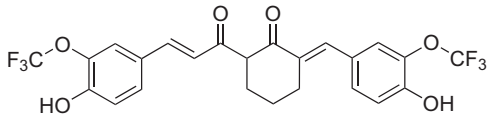	516.39	6.70	N.D.

MW: Molecular weight. *C* log *P*: *C* log *P* values calculated in Chem Draw software. IC_{50}: The half-maximal inhibitory concentrations with regard to ThT fluorescence were used to evaluate binding activities of the curcumin derivatives to Aβ aggregates, which were measured as described in Section 2.

formation of higher molecular size Aβ aggregates when incubated with Aβ during the aggregation state *in vitro* and to cause increasingly lower molecular size Aβ aggregates and possibly reduce cell toxicity [16]. In addition, FMeC1 binds not only to fibrillar Aβ aggregates but also to soluble oligomeric Aβ species [17]. Soluble oligomers rather than monomeric or insoluble fibrillar Aβ aggregates are believed to have a major role in neuronal and synaptic dysfunction in AD [18]. Therefore, it is possible that the interaction of FMeC1 with soluble oligomers reduces toxicity by altering the behavior of the oligomers.

To date, we have synthesized a series of novel curcumin derivatives (called the Shiga-Y series) other than FMeC1 [19]. The purpose of the present study was to identify candidates in our collection that are effective in AD by investigating the inhibitory effects of our curcumin derivatives on Aβ aggregation and the cell toxicities of Aβ aggregates.

2. Materials and methods

2.1. Materials

Curcumin was purchased from Wako (Osaka, Japan). Curcumin derivatives were synthesized as described in Supplementary methods Section. The structures of curcumin and the derivatives are shown in Table 1. In the previous study, we termed SY5 and SY6 as FMeC1 and FMeC2, respectively; however, here we use the original names: SY5 and SY6.

2.2. Preparation of Aβ aggregates

Lyophilized Aβ (1–42) peptide (Peptide Institute, Osaka, Japan) was dissolved in cold 1,1,1,3,3,3-hexafluoro-2-propanol (HFIP; Wako) at 1 mM and incubated at 37 °C for 1 h. The HFIP acts as a hydrogen-bond breaker and is used for eliminating pre-existing structural inhomogeneities in Aβ [20]. An aliquot of the solution containing the dissolved peptide was collected in microcentrifuge tubes, and the HFIP was removed by evaporation. The resulting peptide was stored as a film at −30 °C. Immediately prior to use, the HFIP-pretreated Aβ (1–42) was resuspended to a final concentration of 5 mM in anhydrous dimethyl sulfoxide (DMSO) (Sigma-Aldrich, St. Louis, MO, USA) by pipette mixing followed by vortex mixing. To induce aggregation of Aβ, the 5 mM Aβ (1–42) was diluted to 10 μM in phosphate-buffered saline (PBS), and the solution was incubated for 24 h at 37 °C. To investigate the effects of curcumin and its derivatives on Aβ aggregation, the compounds, which were dissolved to a concentration of 1.5 mM in DMSO, were added to 10 μM Aβ (1–42) to obtain a final concentration of 30 μM. After 24 h of incubation, Aβ was used for cell viability assays and electrophoresis. The concentration of the compounds (30 μM) used in the present study was determined on the basis of the solubility of the compounds and our previous study. Curcumin and the derivatives used in the present study could be dissolved in the above solution at 30 μM, but some were not soluble at 100 μM. In addition, our previous study showed significant inhibition of Aβ aggregation by 30 μM SY5, which indicated that ≥30 μM was high enough to show an inhibitory effect on Aβ aggregation. Therefore, the concentration of 30 μM was selected in the present study. The experimental procedures used such as those used during the incubation with Aβ and in the cell viability assay were performed under dark conditions to protect the compounds from light exposure because curcumin and the derivatives were probably sensitive to light.

2.3. Native gel electrophoresis

Aβ (1–42) samples were diluted to 2.25 μM in native sample buffer (BioRad, Hercules, CA), and 10 μL of each was loaded under native conditions onto 5–20% precast polyacrylamide gels (SuperSep Ace; Wako), electrophoresed in native buffer at 100 V for 4 h at 4 °C, and transferred to PVDF membrane (Immobilon-P; Merck Millipore, Billerica, MA) at 10 V for 1 h. The membrane was subject to Western blotting as described below.

2.4. Sodium dodecyl sulfate polyacrylamide gel electrophoresis (SDS-PAGE) and western blotting

Aβ samples were diluted 4× to 2.25 μM in sample buffer (62.5 mM Tris, pH 6.8, 1% SDS, 25% glycerol) without heating. Samples (10 μL) were separated on 10–20% precast polyacrylamide gels (SuperSep Ace; Wako) and transferred to a polyvinylidene difluoride membrane at 10 V for 1 h. The membranes were blocked with 5% skim milk in Tris-buffered saline (TBS; 25 mM Tris–HCl, pH 7.4, 0.9% NaCl) containing 0.1% Tween 20 (TBS-T), washed for 10 min with TBS-T, and incubated with mouse monoclonal anti-Aβ antibody (1:1000) (clone 6E10; Covance, Princeton, NJ, USA) in TBS-T for 1 h at room temperature. After washing three times for 10 min with TBS-T, the membrane was incubated with horseradish peroxidase-conjugated anti-mouse IgG antibody (1:20,000; Jackson ImmunoResearch, West Grove, PA, USA) in TBS-T containing 0.5% skim milk for 1 h at room temperature. The membranes were then washed three times for 10 min with TBS-T. Immunoreactive proteins were visualized by chemiluminescence (SuperSignal West Pico; Thermo Scientific, Rockford, IL, USA) using

a lumino-image analyzer (LAS-4000; Fujifilm, Tokyo, Japan).

For semi-quantitative analysis, band intensities in the ranges of 15–20, 20–37, 37–75, and 75–200 kDa relative to the marker intensities in SDS-PAGE were measured using image processing software (Image J; National Institutes of Health, Bethesda, MD, USA). The results were expressed as percentages relative to the control condition intensities (Aβ aggregates with DMSO).

2.5. Cell culture

The human neuroblastoma cell line, SH-SY5Y (ATCC, Manassas, VA, USA), was cultured in Dulbecco's modified Eagle's medium/Ham's F-12 (1:1) with L-glutamine, sodium pyruvate, and N-2-hydroxyethylpiperazine-N-2′-ethanesulfonic acid (referred to as HEPES) (Nacalai Tesque, Kyoto, Japan) supplemented with 10% (v/v) fetal bovine serum, 100 μ/mL penicillin, and 100 μg/mL streptomycin, and kept at 37 °C in humidified 5% CO_2/95% air.

2.6. Cell viability

To evaluate cell viability, we performed the 3-(4,5-dimethylthiazol-2-yl)-2,5-diphenyltetrazolium bromide (MTT) assay as an index of surviving cells, according to the instruction manual (MTT Cell Count Kit; Nacalai Tesque). The SH-SY5Y cells were seeded at 5×10^4 cells/well in a 96-well microplate. Twenty-four hours after plating, the culture medium was replaced with 100 μL of fresh medium with or without Aβ and curcumin compounds. After 24 h of incubation at 37 °C in a humidified atmosphere, 10 μL of 5 mg/mL MTT solution was added to the wells, and the cells were incubated for an additional 4 h at 37 °C in a humidified atmosphere. Then, 100 μL of solubilization solution (isopropanol/0.04 mol/L HCl) was added to the well, and the plate was kept overnight at 37 °C in a humidified atmosphere to completely dissolve the formazan. Optical density was then measured in triplicate as technical replicates at 570 nm at a reference wavelength of 700 nm using a microplate reader (Infinite M200; Tecan, Männedorf, Switzerland). Optical density $(OD)_{700}$ values were subtracted from OD_{570} values to obtain corrected OD values, and the cell viability was calculated using the following formula: Cell viability (%)=[(corrected OD of test sample − corrected OD of 100% death control)/(corrected OD of untreated control − corrected OD of 100% death control)] × 100.

We tested cell viability with each of the following compounds in multi-well assay plates: DMSO, curcumin, MR195, SY1, SY2, SY4, SY5, SY6, SY7, SY8, SY9, SY10, SY11, SY12, SY13, SY14, SY15, SY16, SY17, SY18, and SY20. Three wells per plate were assigned to each compound, and optical density was measured in every well, then averaged for each compound on the plate. This set of tests was run three times (that is, in three identical plates) so that three independent three-well experiments were done for each compound, and the optical density measurements were presented as mean ± standard error of the mean (SEM) for each compound. In the same way, we tested cell viability with DMSO, SY21, SY22, SY23, SY26, SY27, SY28, SY29, SY30, SY31, SY32, SY33, SY34, SY35, SY36, SY37, SY38, SY39, SY40, SY41, SY42, and SY43 following the same procedure. The DMSO was used for quality control in both sets of measurements, and so it was tested 6 times, whereas each compound was tested 3 times, at 3 wells per plate.

2.7. Thioflavin T fluorescence assay

The half-maximal inhibitory concentrations (IC_{50}) with regard to Thioflavin T (ThT) fluorescence were used to evaluate binding activities to Aβ aggregates of the curcumin derivatives. ThT was diluted to a concentration of 5 μM in 50 mM glycine–NaOH (pH 8.5), and the solution was stored at room temperature in the dark before use. To measure IC_{50} values, a broad concentration range (12.5 nM–25 μM) using five concentration points of the curcumin derivatives were each mixed with 2 μL of Aβ aggregates in a well of a black 96-well non-binding plate (Greiner Bio-One, Frickenhausen, Germany). Then, 200 μL of 5 mM ThT solution was added to each well. The fluorescence of ThT was measured using a FlexStation (Molecular Devices, Sunnyvale, CA, USA) at an excitation wavelength of 440 nm, an emission wavelength of 490 nm, and a cut off wavelength of 475 nm. The IC_{50} values were estimated using GraphPad Prism (GraphPad Software, La Jolla, CA, USA).

2.8. Statistical analysis

The results were presented as mean ± standard error of the mean (SEM) of at least three independent experiments. Statistical significance was determined by one-way analysis of variance (ANOVA) followed by the Dunnett post hoc test for multiple comparisons (GraphPad Prism 6; GraphPad Software).

3. Results

3.1. Changes in the profiles of Aβ (1–42) aggregates formed in the presence of curcumin derivatives

We investigated the solubility of curcumin and several derivatives which we prepared including SY5, SY12, SY28, SY31, and SY33. Thus, we prepared 1.5 mM curcumin and its derivatives in 100% DMSO as stock solutions. Then, the solutions were diluted with 10 μM PBS (containing 2% DMSO) to make 30 μM final concentrations. We obtained a clear yellowish-orange solution in each case. Then, we further confirmed absence of precipitation in two ways. First, we looked for any precipitate from each solution by light microscopy, as follows. Two microliters of the solution were transferred to a glass slide, which was covered with a slip. When we looked at the slides through a light microscope, we observed no precipitation in any sample. However, when we made 200 μM curcumin solution, we clearly observed precipitates from the solution. Next, we looked for precipitates from the solutions after centrifugation at 50,000 rpm (104,300*g*) for 60 min at 20 °C. No precipitates were observed in the bottom of any samples.

We performed electrophoresis to evaluate the profiles of Aβ (1–42) prepared by incubation with curcumin and the derivatives for 24 h at 37 °C. In native-PAGE analysis, Aβ (1–42) prepared by incubating with DMSO for 24 h at 37 °C showed a band predominantly at the top of the gel, which indicated the formation of Aβ aggregates (Fig. 1A). There were marked smear bands in Aβ (1–42) prepared with the compounds for 24 h. The smear bands indicated formation of lower molecular weight Aβ aggregates and oligomers. The SDS-PAGE profiles showed an increase in monomers, trimers, and tetramers as well as in the smear bands in Aβ (1–42) prepared with the compounds for 24 h relative to those in the Aβ (1–42) aggregates formed in the presence of vehicle control (Fig. 1B). Comparison of the bands between native- and SDS-PAGE showed that monomers, trimers, and tetramers that did not appear by native-PAGE were detected by SDS-PAGE, which suggested that these Aβ species were generated by the disassembly of aggregates derived from SDS processing during sample preparation. In contrast, Aβ (1–42) products prepared with the compounds that showed many smear bands in native-PAGE tended to give many smear bands in SDS-PAGE, which suggested that the smear bands of Aβ (1–42) in SDS-PAGE could be indicative of the formation of lower molecular weight Aβ aggregates under native conditions.

In semi-quantitative analysis, SY5, SY12, SY15, SY26, SY28, and SY33 showed significant increases in the densities of the bands of

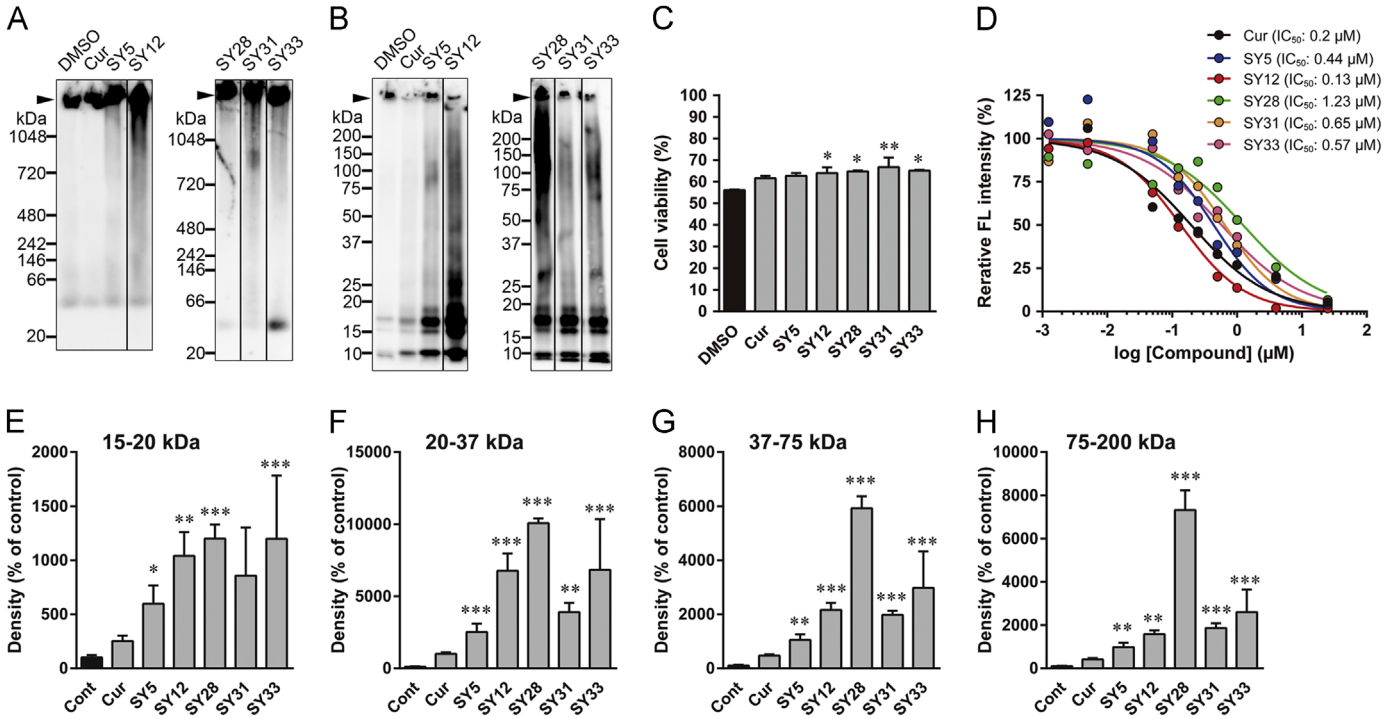

Fig. 1. Effect of selected curcumin derivatives on the aggregation of Aβ (1–42). Representative SDS-PAGE (A) and native-PAGE (B) profiles of Aβ (1–42) prepared by incubating with DMSO as the vehicle control, curcumin (Cur), SY5, SY12, SY28, SY31, and SY33 for 24 h at 37°C. Marked smear bands were observed for SY5, SY12, SY28, SY31, and SY33 treated Aβ (1–42) in both SDS-PAGE (A) and native-PAGE (B). Gel images of Aβ prepared with DMSO, Cur, SY5, and SY12 were taken from one gel, and gel images of Aβ prepared with SY28, SY31, and SY33 were taken from another gel. Arrowheads in (A) and (B) indicate the position of the top of the gel. (C) Cell viability was measured in SH-SY5Y cells at 24 h after exposure to Aβ (1–42) prepared with DMSO as the vehicle control, curcumin (Cur), SY5, SY12, SY28, SY31, and SY33. Data are the means ± SEMs of at least three independent experiments. Significance (Dunnet post-test after ANOVA): $*p < 0.05$, $**p < 0.01$ vs. DMSO. The values of cell viability in all compounds measured in the present study are presented in Table 2. (D) Competition curves for Cur, SY5, SY12, SY28, SY31, and SY33 in the Thioflavin T (ThT) competition study. The half-maximal inhibitory concentrations (IC50) with regard to ThT fluorescence were used to evaluate binding activities of the curcumin derivatives to Aβ aggregates. The IC50 values in all compounds measured in the present study are listed in Table 2. (E-H) Band intensities in the ranges of 15–20 (E), 20–37 (F), 37–75 (G), and 75–200 kDa (H) were measured by SDS-PAGE for semi-quantitative analysis of Aβ (1–42) prepared by incubating with DMSO as the vehicle control, curcumin (Cur), SY5, SY12, SY28, SY31, and SY33. Data are the means ± SEMs of at least three independent experiments. Significance (Dunnet post-test after ANOVA): $*p < 0.05$, $**p < 0.01$, $***p < 0.001$, vs. DMSO. The values of the band intensities for all compounds measured in the present study are listed in Table 2.

Aβ (1–42) in all ranges of 15–20, 20–37, 37–75, and 75–200 kDa relative to those of Aβ (1–42) prepared with vehicle control (DMSO) (Table 2). SY14, SY31, and SY34 showed significant increases in the densities in the ranges of 37–75 and 75–200 kDa (Table 2). In addition, there were significant increases in the densities only in the ranges of 15–20 kDa for SY2, 20–37 kDa for SY37 and SY38, and 75–200 kDa for SY43 (Table 2). Taken together, 14 of 41 compounds showed a significant increase in the densities of the bands of Aβ (1–42) by incubation during the aggregation process relative to those of Aβ (1–42) prepared in the presence of the vehicle control.

3.2. Effect of curcumin derivatives on cell toxicity of Aβ aggregates

We investigated the cell toxicity of Aβ (1–42) incubated with curcumin and its derivatives during the aggregation process. To evaluate cell viability, Aβ (1–42) prepared by incubating at a concentration of 10 μM for 24 h at 37 °C in the presence of 30 μM curcumin derivatives was treated in SH-SY5Y cells for 24 h at final concentrations of 0.3 μM Aβ (1–42) and 0.9 μM curcumin derivatives. Significantly higher cell viability was observed following exposure to Aβ (1–42) incubated with SY12, SY28, SY31, SY32, and SY33 during the aggregation process, than following exposure to Aβ (1–42) incubated with vehicle control ($p < 0.05$ for SY12, SY28, SY32, and SY33; $p < 0.01$ for SY31) (Viability A in Table 1). We next investigated the effect of simultaneous treatment with 0.9 μM curcumin derivatives and 0.3 μM Aβ (1–42) aggregates. Simultaneous treatment did not improve cell viability 24 h after exposure to Aβ (1–42) aggregates, but there was significant reduction in cell viability by simultaneous treatment with SY4 relative to that by treatment with the vehicle control ($p < 0.05$; Viability B in Table 1). We further evaluated cell viability 24 h after treatment with 0.9 μM curcumin derivatives alone. There was no significant difference in cell viability after treatment with curcumin derivatives alone except for SY14 and SY18; these two compounds significantly reduced cell viability ($p < 0.05$ for SY14; $p < 0.001$ for SY18) (Viability C in Table 2).

3.3. Correlation of cell viability and increased density in SDS-PAGE

We investigated whether there were correlations between cell viabilities after exposure to Aβ (1–42) incubated with the compounds for 24 h, and the densities of the SDS-PAGE bands of Aβ (1–42) incubated with the compounds. Significant positive correlations were observed between the cell viabilities and densities in all ranges of 15–20 (Fig. 2A; Pearson's $r = 0.461$; $p < 0.001$), 20–37 (Fig. 2B; Pearson's $r = 0.535$; $p < 0.001$), 37–75 (Fig. 2C; Pearson's $r = 0.478$; $p < 0.01$), and 75–200 kDa (Fig. 2D; Pearson's $r = 0.427$; $p < 0.01$) (Fig. 2). Significant positive correlations were also observed between the cell viabilities and ClogP values of the curcumin derivatives (Pearson's $r = 0.474$; $p < 0.01$) (Fig. 2). In contrast, there were no correlations between the molecular weights of the curcumin derivatives and cell viabilities (Pearson's $r = 0.069$; $p = 0.666$) or between the IC_{50} values and cell viabilities (Pearson's $r = -0.096$; $p = 0.612$) (data not shown).

Table 2
Comparison of densities determined by SDS-PAGE and of cell viabilities

Name	Density					Viability					
						A. Exposure to Aβ pre-incubated with the compounds		B. Simultaneous treatment with Aβ aggregates and the compounds		C. Compound alone	
	n	15–20 kDa (%)	20–37 kDa (%)	37–75 kDa (%)	75–200 kDa (%)	*n*	%	*n*	%	*n*	%
DMSO	14	100 ± 23	100 ± 41	100 ± 27	100 ± 23	6	56.1 ± 1.1	6	54.0 ± 0.9	6	102.7 ± 3.5
Cur	14	253 ± 50	1012 ± 103	472 ± 49	414 ± 64	3	61.6 ± 1.7	3	53.5 ± 1.5	3	97.5 ± 7.3
MR195	5	343 ± 161	1411 ± 539	618 ± 183	437 ± 100	3	60.9 ± 2.1	3	56.5 ± 2.3	3	97.1 ± 6.7
SY1	3	534 ± 410	1350 ± 641	606 ± 154	463 ± 87	3	58.8 ± 1.9	3	51.2 ± 1.7	3	103.3 ± 2.2
SY2	3	1189 ± 634***	2454 ± 817	1024 ± 264	965 ± 214	3	58.5 ± 1.4	3	50.4 ± 3.6	3	101.4 ± 2.0
SY4	3	281 ± 86	636 ± 135	389 ± 37	217 ± 31	3	52.9 ± 0.7	3	45.6 ± 2.6*	3	91.6 ± 3.2
SY5	14	598 ± 170*	2521 ± 588***	1047 ± 212**	981 ± 209**	3	62.7 ± 1.3	3	54.6 ± 1.5	3	102.2 ± 3.6
SY6	3	103 ± 25	225 ± 118	220 ± 61	200 ± 52	3	57.7 ± 1.6	3	55.1 ± 3.0	3	99.4 ± 2.2
SY7	5	301 ± 78	1444 ± 429	564 ± 94	473 ± 71	3	59.7 ± 1.8	3	55.3 ± 3.0	3	102.5 ± 2.0
SY8	3	179 ± 36	1425 ± 211	913 ± 119	825 ± 65	3	59.3 ± 1.7	3	48.2 ± 2.1	3	91.8 ± 3.7
SY9	3	54 ± 22	74 ± 55	125 ± 23	97 ± 4	3	53.2 ± 1.2	3	50.7 ± 3.2	3	94.2 ± 2.5
SY10	3	247 ± 141	1416 ± 454	666 ± 177	575 ± 125	3	60.5 ± 2.4	3	52.1 ± 2.2	3	92.9 ± 1.7
SY11	3	331 ± 138	1839 ± 607	905 ± 331	805 ± 253	3	60.8 ± 2.3	3	52.9 ± 2.5	3	98.2 ± 2.0
SY12	3	1040 ± 220**	6768 ± 1205***	2162 ± 263***	1579 ± 178**	3	64.0 ± 2.8*	3	51.9 ± 2.3	3	91.6 ± 2.3
SY13	5	536 ± 170	2407 ± 610	1203 ± 280*	1030 ± 185*	3	63.6 ± 2.2	3	57.5 ± 1.6	3	96.2 ± 2.9
SY14	3	768 ± 307	4393 ± 1906***	2126 ± 1014***	1750 ± 927 ***	3	59.8 ± 2.0	3	50.6 ± 2.0	3	84.5 ± 1.7*
SY15	3	991 ± 405*	5109 ± 1379***	2079 ± 609***	2002 ± 450***	3	60.1 ± 2.2	3	52.1 ± 2.4	3	90.9 ± 0.8
SY16	3	85 ± 11	534 ± 134	216 ± 64	161 ± 30	3	57.9 ± 2.3	3	51.3 ± 1.6	3	94.1 ± 2.8
SY17	3	304 ± 173	786 ± 316	479 ± 189	524 ± 277	3	62.2 ± 2.6	3	53.2 ± 2.1	3	94.1 ± 2.2
SY18	3	98 ± 30	239 ± 66	183 ± 12	155 ± 12	3	58.5 ± 2.3	3	49.6 ± 3.1	3	69.5 ± 7.7***
SY20	3	203 ± 93	984 ± 292	586 ± 191	548 ± 126	3	62.4 ± 2.3	3	54.8 ± 1.5	3	89.0 ± 12.7
SY21	5	144 ± 28	363 ± 104	341 ± 71	342 ± 73	3	58.8 ± 2.0	3	50.5 ± 0.4	3	96.7 ± 1.7
SY22	3	234 ± 90	626 ± 365	437 ± 96	457 ± 86	3	59.3 ± 2.6	3	50.5 ± 0.7	3	95.8 ± 3.6
SY23	3	380 ± 141	1311 ± 489	607 ± 234	501 ± 204	3	58.2 ± 2.3	3	52.6 ± 1.1	3	97.9 ± 2.4
SY26	3	1195 ± 489***	5622 ± 1637***	2170 ± 488***	2442 ± 376***	3	60.1 ± 1.4	3	54.3 ± 0.9	3	97.6 ± 1.6
SY27	3	299 ± 87	1120 ± 156	639 ± 177	556 ± 58	3	60.8 ± 1.8	3	53.3 ± 0.2	3	98.5 ± 5.3
SY28	3	1201 ± 129***	10082 ± 326***	5933 ± 438***	7326 ± 908***	3	64.8 ± 0.4*	3	54.6 ± 0.9	3	95.9 ± 3.1
SY29	3	323 ± 127	1081 ± 223	520 ± 85	652 ± 112	3	58.0 ± 1.7	3	52.6 ± 1.5	3	99.6 ± 6.2
SY30	3	248 ± 156	1261 ± 700	632 ± 282	570 ± 231	3	62.2 ± 1.8	3	53.7 ± 1.8	3	98.6 ± 3.1
SY31	3	857 ± 447	3911 ± 635**	1976 ± 151***	1861 ± 227***	3	66.8 ± 2.0**	3	55.3 ± 1.2	3	94.2 ± 4.1
SY32	3	284 ± 179	1281 ± 648	686 ± 292	614 ± 174	3	64.7 ± 2.1*	3	54.1 ± 2.4	3	98.2 ± 3.6
SY33	3	1199 ± 584***	6849 ± 3510***	2976 ± 1352***	2606 ± 1036***	3	65.1 ± 1.8*	3	53.8 ± 0.8	3	97.8 ± 4.2
SY34	3	877 ± 84	6386 ± 900***	3816 ± 705***	3058 ± 854***	3	59.1 ± 2.4	3	53.9 ± 1.4	3	94.1 ± 3.4
SY35	3	185 ± 32	281 ± 54	289 ± 36	294 ± 25	3	50.9 ± 1.5	3	51.6 ± 1.7	3	93.7 ± 2.9
SY36	3	122 ± 47	117 ± 78	211 ± 35	304 ± 53	3	55.2 ± 1.1	3	51.1 ± 1.3	3	96.1 ± 5.4
SY37	3	689 ± 171	3945 ± 784**	1473 ± 377	1430 ± 285	3	60.3 ± 1.5	3	53.0 ± 1.5	3	93.0 ± 4.1
SY38	3	490 ± 122	3187 ± 853*	1295 ± 384	1032 ± 313	3	62.9 ± 2.1	3	51.1 ± 1.6	3	91.6 ± 3.9
SY39	3	270 ± 128	348 ± 127	265 ± 44	398 ± 37	3	50.6 ± 1.5	3	51.8 ± 1.2	3	94.7 ± 6.7
SY40	3	231 ± 72	244 ± 110	275 ± 63	345 ± 75	3	53.6 ± 1.6	3	52.2 ± 0.9	3	95.2 ± 6.0
SY41	3	301 ± 84	1584 ± 115	728 ± 164	949 ± 147	3	61.9 ± 1.7	3	55.9 ± 0.4	3	93.4 ± 5.9
SY42	3	132 ± 17	427 ± 209	263 ± 104	313 ± 98	3	60.8 ± 1.8	3	53.6 ± 0.8	3	88.6 ± 6.3
SY43	3	357 ± 103	1457 ± 119	945 ± 135	1585 ± 488**	3	57.6 ± 2.0	3	56.0 ± 0.9	3	89.7 ± 5.0

Density: Aβ samples prepared by incubating with curcumin and the derivatives for 24 h at 37 °C were subjected to SDS-PAGE followed by Western blotting. The densities of the bands in the ranges of 15–20, 20–37, 37–75, and 75–100 kDa were then measured by using Image J. Viability (A): Cell viabilities after exposure to Aβ incubated with the compounds for 24 h at 37 °C; Viability (B): Cell viabilities after simultaneous treatment with Aβ aggregates and the compounds; and Viability (C): Cell viabilities after treatment with the compounds alone. The results are presented as means ± SEMs of at least three independent experiments. Statistical significance was determined by one-way analysis of variance followed by the Dunnett post hoc test for multiple comparisons.
Significance (Dunnet post-test after ANOVA): *$p < 0.05$, **$p < 0.01$. ***$p < 0.001$ vs. DMSO.

4. Discussion

In this study, we investigated the effects of our curcumin derivatives on Aβ aggregation and its cell toxicity. According to the SDS-PAGE profiles, 14 of 41 compounds showed significant increases in the densities of the bands of Aβ (1–42) by incubation during the aggregation process relative to those of Aβ (1–42) prepared in the presence of the vehicle control. Among the compounds, SY12, SY28, SY31, and SY33 also reduced the cell toxicities of the Aβ aggregates by incubation during the aggregation process. Taking these findings together, we propose SY12, SY28, SY31, and SY33 as therapeutic candidates for preventing AD.

Several reports have shown the potential of curcumin derivatives for modulating Aβ metabolism [21–24], antioxidative stress, and cancer prevention [25,26]. Reinke and Gestwicki outlined the optimal linker length and flexibility (or rigidity) of two phenyl groups of curcumin, for inhibition of Aβ aggregation [24]. In addition, they proposed that hydroxy substitutions on the aromatic end groups are required for inhibition [24]. In the present study, our candidate compounds fit the model proposed by Reinke and Gestwicki [24]. Furthermore, the effect of a curcumin derivative with a 1,7-bis (4′-hydroxy-3′-trifluoromethoxyphenyl) group (SY5) was stronger than that of a curcumin derivative with a 1,7-bis (4′-hydroxy-3′-methoxyphenyl) group (SY23), which suggested that trifluoromethoxy groups on aromatic rings are favorable groups for inhibiting Aβ aggregation. In addition, curcumin derivatives that showed effects on Aβ aggregation had at least one hydroxy group on the aromatic groups in their structure. In contrast, curcumin derivatives without hydroxy groups on the aromatic groups (SY7, SY8, SY9, SY18, SY21, SY22, SY42) showed no effects on Aβ aggregation. Although, curcumin derivatives

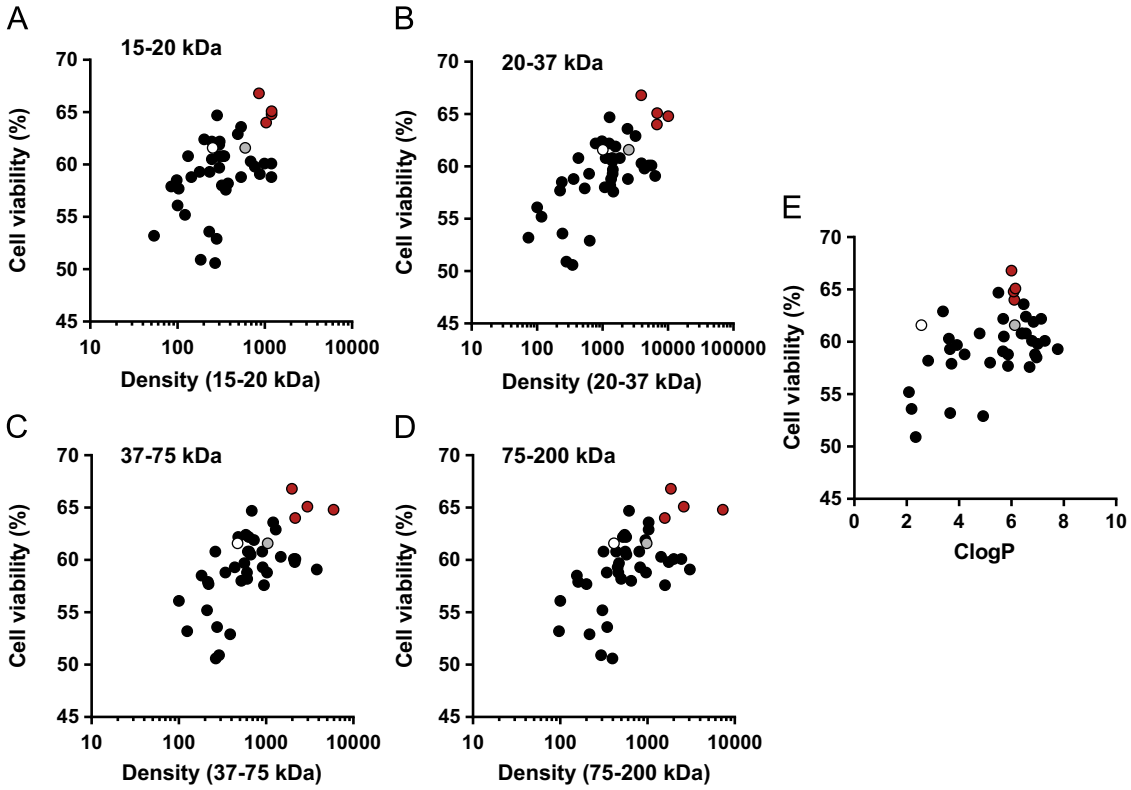

Fig. 2. Positive correlations between the cell viabilities and densities of Aβ in SDS-PAGE or ClogP values. (A-D) Significant positive correlations were observed between the cell viabilities after exposure to Aβ (1–42) prepared with the compounds and the densities of the bands of Aβ (1–42) in the ranges of 15–20 (A; Pearson's r = 0.461; $p < 0.001$), 20–37 (B; Pearson's r = 0.535; $p < 0.001$), 37–75 (C; Pearson's r = 0.478; $p < 0.01$), and 75–200 kDa (D; Pearson's r = 0.427; $p < 0.01$). (E) Positive correlations between cell viabilities and ClogP values (Pearson's r = 0.474; $p < 0.01$) were observed. Curcumin, SY5, and selected compounds (SY12, SY28, SY31, and SY33) are indicated by open circles, gray circles and red circles, respectively.

without hydroxy groups on the aromatic groups have been reported to exert higher inhibitory effects on Aβ oligomerization than curcumin [23], according to our results and the above model proposed by Reinke and Gestwicki, we assumed that the hydroxy groups on the aromatic groups in curcumin derivatives are essential for inhibiting Aβ aggregation. Furthermore, the curcumin derivatives that we propose here, SY12, SY28, SY31, and SY33, have substituents at the C-4 position. Taken together, we assumed that the combination of 1,7-bis (4′-hydroxy-3′-trifluoromethoxyphenyl) groups and a suitable substituent at the C-4 position were key influences on the therapeutic effect of curcumin derivatives.

We previously reported significant improvement of cell viability by incubation of SY5 (FMeC1) with Aβ (1–42) aggregates during the aggregation process [16]. In the present study, we observed a marked increase in cell viability following incubation of SY5 (FMeC1; Viability A in Table 1), as in the previous study. However, we could not detect statistically significant differences in any improvements in cell viability, presumably because of the lower power of the statistical analysis that we used. The power of the test is reduced when the number of groups compared is increased. Thus, even if a large increase in cell viability was observed after the treatment, it was difficult to assign statistical significance when we compared 42 compounds at once.

Previous studies have demonstrated that curcumin can bind to β-sheeted structures in Aβ fibrils and inhibit further elongation of the fibrillar structures [11,12]. Furthermore, Yang et al. [12] also showed inhibition of Aβ oligomer formation by curcumin. Therefore curcumin and its derivatives may inhibit both Aβ oligomerization and fibrillogenesis. However, it was difficult to know the exact sizes of the Aβ aggregates and oligomers that we prepared in the present study; thus, we could not investigate the mechanisms of inhibition of Aβ oligomerization.

In the SDS-PAGE analysis, we measured the densities of the bands. Interestingly, SY2 treatment induced significant increases in the densities of the band corresponding to trimers and tetramers of 15–20 kDa, but not in the other band ranges. However, Aβ aggregates that were formed with SY2 did not enhance the toxicity of the Aβ aggregates. In addition, native-PAGE analysis showed almost no bands corresponding to trimers and tetramers of 15–20 kDa. These findings suggest that the bands of trimers and tetramers in SDS-PAGE might not reflect the appearance of these species in real samples; therefore, these compounds may not be responsible for increasing cell toxicity.

It is difficult to dissolve curcumin in an aqueous solution because of poor solubility. In the present study, we prepared 1.5 mM curcumin and our derivatives in DMSO as stock solutions. Then, the solutions were diluted in 10 μM in PBS (with 2% DMSO) at a final concentration of 30 μM. Thus, 4% DMSO was present in the final reaction mixtures and would have contributed to dissolving the compounds in the solutions. In addition, several studies have reported using >30 μM curcumin in aqueous solutions [11,12,24]. Thus, we thought that the use of curcumin at 30 μM was reasonable to investigate its effects.

There were significant positive correlations between the cell viabilities and densities in the ranges of 15–20, 20–37, 37–75, and 75–200 kDa in the SDS-PAGE profiles after exposure to Aβ aggregates incubated with curcumin derivatives. Thus, it is likely that curcumin derivatives with higher inhibitory effects on Aβ aggregation contribute to increasing cell viability, which suggests that Aβ species were formed in our experiments with compounds that had weaker cell toxicity. In addition, our results indicated that the *C* log *P* values of the curcumin derivatives were also involved in the effects *via* unknown mechanisms. Further study is needed to elucidate the mechanisms underlying the effects of the curcumin derivatives.

It has been reported that curcumin is apparently a highly

pleiotropic molecule that physically interacts with numerous targets [5]. Curcumin binds to proteins such as P-glycoprotein, multidrug-resistance proteins 1 and 2, glutathione, protein kinase C, ATPase, ErbB2, and alpha1-acid glycoprotein and inhibits the activation of various transcription factors and expression of growth- and metastasis-promoting genes and also downregulates the activity of multiple kinases. The dicarbonyl unit is one of the causative moieties of curcumin because molecules containing a β-diketone are known to form stable complexes with multivalent metal cations [27]. For example, curcumin forms chelates with metals such as boron, copper, aluminum, magnesium, zinc, lead, cadmium, and ferrous (Fe^{2+}) and ferric (Fe^{3+}) iron as well as with metal oxides such as vanadyl and nonmetals such as selenium. These interactions are often beneficial for anti-inflammatory effects, anti-tumor effects, and anti-AD effects. On the other hand, the interactions of curcumin with essential molecules for life could cause off-target toxicity, as shown by three compounds (SY4, SY14, SY18) in the present study. Although we did not investigate the off-target toxicity induced by the curcumin derivatives in detail in this study, it would be very useful to understand the mechanisms of the off-target toxicity to develop curcumin derivatives as therapeutic drugs for AD.

There were potential weaknesses in the present study. First, only an *in vitro* study was conducted to probe the effect of the compounds. Senile plaques consist of not only Aβ aggregates but also of various proteins and metals. Therefore, the Aβ aggregates used in this study might have been highly artificial. Second, more detailed investigations regarding the inhibition of Aβ oligomer formation is required to elucidate the mechanisms of the effects of the compounds. Finally, there was little evidence of structure–function relationships of the compounds. As a future research direction, an *in vivo* study using an animal model of AD and including experiments focused on inhibition of Aβ oligomer formation by the compounds should be conducted with candidates selected on the basis of the results of the present study. An additional goal would be to elucidate the structure–function relationships of the compounds.

5. Conclusions

We propose SY12, SY28, SY31, and SY33 as curcumin derivatives that may prevent AD. These curcumin derivatives exhibited high inhibitory effects on Aβ aggregation and induced formation of lower molecular size Aβ species with weaker cell toxicities. We expect that these compounds will exert therapeutic effects that prevent AD in future *in vivo* studies.

Conflict of interest

Shiga University of Medical Science has applied for patents (JP2012/260046) for the compounds, with D. Yanagisawa, H. Taguchi, and I. Tooyama named as the inventors.

Acknowledgments

This study was supported by Grants-in-Aid for Scientific Research (B) (JSPS KAKENHI Grant number 26290022) (I.T.); for Scientific Research (C) (15K01282) (H.T.); and for a Young Scientist (B) (15K16321) (D.Y.) from the Japan Society for the Promotion of Science (JSPS); and by a Grant-in-Aid for Scientific Research on Innovative Areas ('Brain Environment') (MEXT KAKENHI Grant number 26640042) (I.T.) from the Ministry of Education, Science, Sports, and Culture of Japan (MEXT).

Appendix A. Supplementary material

Supplementary data associated with this article can be found in the online version at http://dx.doi.org/10.1016/j.bbrep.2015.10.009.

References

[1] M. Citron, Alzheimer's disease: strategies for disease modification, Nat. Rev. Drug Discov. 9 (2010) 387–398.
[2] H.W. Querfurth, F.M. LaFerla, Alzheimer's disease, N. Engl. J. Med. 362 (2010) 329–344.
[3] J. Hardy, D.J. Selkoe, The amyloid hypothesis of Alzheimer's disease: progress and problems on the road to therapeutics, Science 297 (2002) 353–356.
[4] C.R. Jack, D.S. Knopman, W.J. Jagust, L.M. Shaw, P.S. Aisen, M.W. Weiner, R. C. Petersen, J.Q. Trojanowski, Hypothetical model of dynamic biomarkers of the Alzheimer's pathological cascade, Lancet Neurol. 9 (2010) 119–128.
[5] A. Goel, A.B. Kunnumakkara, B.B. Aggarwal, Curcumin as "Curecumin": from kitchen to clinic, Biochem. Pharmacol. 75 (2008) 787–809.
[6] A.N. Begum, M.R. Jones, G.P. Lim, T. Morihara, P. Kim, D.D. Heath, C.L. Rock, M. A. Pruitt, F. Yang, B. Hudspeth, S. Hu, K.F. Faull, B. Teter, G.M. Cole, S. A. Frautschy, Curcumin structure–function, bioavailability, and efficacy in models of neuroinflammation and Alzheimer's disease, J. Pharmacol. Exp. Ther. 326 (2008) 196–208.
[7] M. Garcia-Alloza, L.A. Borrelli, A. Rozkalne, B.T. Hyman, B.J. Bacskai, Curcumin labels amyloid pathology in vivo, disrupts existing plaques, and partially restores distorted neurites in an Alzheimer mouse model, J. Neurochem. 102 (2007) 1095–1104.
[8] T. Hamaguchi, K. Ono, A. Murase, M. Yamada, Phenolic compounds prevent Alzheimer's pathology through different effects on the amyloid-beta aggregation pathway, Am. J. Pathol. 75 (2009) 2557–2565.
[9] G.P. Lim, T. Chu, F. Yang, W. Beech, S.A. Frautschy, G.M. Cole, The curry spice curcumin reduces oxidative damage and amyloid pathology in an Alzheimer transgenic mouse, J. Neurosci. 21 (2001) 8370–8377.
[10] Q.L. Ma, F. Yang, E.R. Rosario, O.J. Ubeda, W. Beech, D.J. Gant, P.P. Chen, B. Hudspeth, C. Chen, Y. Zhao, H.V. Vinters, S.A. Frautschy, G.M. Cole, Beta-amyloid oligomers induce phosphorylation of tau and inactivation of insulin receptor substrate via c-Jun N-terminal kinase signaling: suppression by omega-3 fatty acids and curcumin, J. Neurosci. 29 (2009) 9078–9089.
[11] K. Ono, K. Hasegawa, H. Naiki, M. Yamada, Curcumin has potent anti-amyloidogenic effects for Alzheimer's beta-amyloid fibrils in vitro, J. Neurosci. Res. 75 (2004) 742–750.
[12] F. Yang, G.P. Lim, A.N. Begum, O.J. Ubeda, M.R. Simmons, S.S. Ambegaokar, P. P. Chen, R. Kayed, C.G. Glabe, S.A. Frautschy, G.M. Cole, Curcumin inhibits formation of amyloid beta oligomers and fibrils, binds plaques, and reduces amyloid in vivo, J. Biol. Chem. 280 (2004) 5892–5901.
[13] D. Yanagisawa, N. Shirai, T. Amatsubo, H. Taguchi, K. Hirao, M. Urushitani, S. Morikawa, T. Inubushi, M. Kato, F. Kato, K. Morino, H. Kimura, I. Nakano, C. Yoshida, T. Okada, M. Sano, Y. Wada, K. Wada, A. Yamamoto, I. Tooyama, Relationship between the tautomeric structures of curcumin derivatives and their Aβ-binding activities in the context of therapies for Alzheimer's disease, Biomaterials 31 (2010) 4179–4185.
[14] R. McClure, D. Yanagisawa, D. Stec, D. Koktysh, D. Xhillari, R. Jaeger, E. Chekmenev, I. Tooyama, J.C. Gore, W. Pham, Inhalable curcumin: offering the potential for translation to imaging and treatment of Alzheimer's disease, J. Alzheimers Dis. 44 (2015) 283–295.
[15] D. Yanagisawa, T. Amatsubo, S. Morikawa, H. Taguchi, M. Urushitani, N. Shirai, K. Hirao, A. Shiino, T. Inubushi, I. Tooyama, In vivo detection of amyloid β deposition using ^{19}F magnetic resonance imaging with a ^{19}F-containing curcumin derivative in a mouse model of Alzheimer's disease, Neuroscience 184 (2011) 120–127.
[16] D. Yanagisawa, N.F. Ibrahim, H. Taguchi, S. Morikawa, K. Hirao, N. Shirai, T. Sogabe, I. Tooyama, Curcumin derivative with the substitution at C-4 position, but not curcumin, is effective against amyloid pathology in APP/PS1 mice, Neurobiol. Aging 36 (2015) 201–210.
[17] D. Yanagisawa, H. Taguchi, A. Yamamoto, N. Shirai, K. Hirao, I. Tooyama, Curcuminoid binds to amyloid-β 1–42 oligomer and fibril, J. Alzheimers Dis. 24 (Suppl. 2) (2011) S33–S42.
[18] C. Haass, D.J. Selkoe, Soluble protein oligomers in neurodegeneration: lessons from the Alzheimer's amyloid β-peptide, Nat. Rev. Mol. Cell Biol. 8 (2007) 101–112.
[19] H. Taguchi, D. Yanagisawa, S. Morikawa, K. Hirao, N. Shirai, I. Tooyama, Synthesis and tautomerism of curcumin derivatives and related compounds, Aust. J. Chem. 68 (2015) 224–229.
[20] W.B. Stine, K.N. Dahlgren, G.A. Krafft, M.J. LaDu, In vitro characterization of conditions for amyloid-beta peptide oligomerization and fibrillogenesis, J. Biol. Chem. 278 (2003) 11612–11622.
[21] S. Gagliardi, S. Ghirmai, K.J. Abel, M. Lanier, S.J. Gardai, C. Lee, J.R. Cashman, Evaluation in vitro of synthetic curcumins as agents promoting monocytic gene expression related to β-amyloid clearance, Chem. Res. Toxicol. 25 (2012) 101–112.
[22] R. Narlawar, K. Baumann, R. Schubenel, B. Schmidt, Curcumin derivatives inhibit or modulate beta-amyloid precursor protein metabolism, Neurodegener. Dis. 4 (2007) 88–93.
[23] R.A. Orlando, A.M. Gonzales, R.E. Royer, L.M. Deck, D.L. Vander Jagt, A chemical

analog of curcumin as an improved inhibitor of amyloid Abeta oligomerization, PLoS One 7 (2012) e31869.
[24] A.A. Reinke, J.E. Gestwicki, Structure–activity relationships of amyloid beta-aggregation inhibitors based on curcumin: influence of linker length and flexibility, Chem. Biol. Drug Des. 70 (2007) 206–215.
[25] E. Ferrari, F. Pignedoli, C. Imbriano, G. Marverti, V. Basile, E. Venturi, M. Saladini, Newly synthesized curcumin derivatives: crosstalk between chemico-physical properties and biological activity, J. Med. Chem. 54 (2011) 8066–8077.
[26] M. Mimeault, S.K. Batra, Potential applications of curcumin and its novel synthetic analogs and nanotechnology-based formulations in cancer prevention and therapy, Chin. Med. 6 (2011) 31.
[27] M. Heger, R.F. van Golen, M. Broekgaarden, M.C. Michel, The molecular basis for the pharmacokinetics and pharmacodynamics of curcumin and its metabolites in relation to cancers, Pharmacol. Rev. 66 (2014) 222–307.